Anisotropy in the irreversible behavior of pointlike defects and twins in $YBa_2Cu_3O_{7-\delta}$ single crystals with a peak effect

H. Küpfer
Forschungszentrum Karlsruhe, Institut für Technische Physik, Postfach 3640, D-76021 Karlsruhe, Germany

A. A. Zhukov
Department of Physics, Moscow State University, Moscow 117234, Russia

A. Will, W. Jahn, R. Meier-Hirmer, and Th. Wolf
Forschungszentrum Karlsruhe, Institut für Technische Physik, Postfach 3640, D-76021 Karlsruhe, Germany

V. I. Voronkova
Department of Physics, Moscow State University, Moscow 117234, Russia

M. Kläser
Universität Karlsruhe, Fakultät für Physik, D-76128 Karlsruhe, Germany

K. Saito
Laboratorium für Festkörperphysik, Eidgenössische Technische Hochschule Hönggerberg, CH-8093 Zürich, Switzerland
(Received 15 November 1995; revised manuscript received 5 February 1996)

In different $RBa_2Cu_3O_{7-\delta}$ (R=Y,Tm) single crystals the peak of the current density j vs magnetic field B is investigated in the angular region B parallel and perpendicular to the c axis of the crystals. The magnetic moment from the current is measured as a function of angle ϕ between field direction and c axis with a vibrating sample magnetometer up to $B=7$ T. The peak effect which probably results from an isotropic pointlike defect structure (oxygen vacancies, impurities from doping or crucible) is observed in $B\|c$ for the current parallel to the a,b plane ($j\|a,b$) and in $B\|a,b$ for both currents $j\|a,b$ and $j\|c$. This was verified in twinned and twin-free crystals. For $B\|c$ the influence of the twin structure on the $j(B)$ peak results in an increase of j below and above the peak from pinning at twin walls. However, in the peak region the current becomes depressed either from channeling of vortices along twin walls or from enhanced stiffness of the tilt modulus of the flux lattice. The twinned crystals show a cusplike dependence of the irreversibility field B_{irr} vs ϕ with the maximum at $B\|c$ in agreement with a Bose-glass transition. Whereas the detwinned crystal reveals a minimum of $B_{irr}(\phi)$ at $B\|c$ as expected from an anisotropic but homogeneous crystal. This interference between pointlike and correlated disorder in the flux lattice becomes less pronounced with larger impurity contents. In $B\|a,b$ intrinsic pinning from CuO layers is observed by an increase of the magnetic moment vs ϕ. This is further proved by lock-in oscillations which demonstrate the matching condition between crystal layer and flux lattice spacing. At higher fields the moment vs ϕ shows an unusual decrease in an angular region $\pm 0.3°$ from $B\|a,b$. This behavior is related to $j\|c$ which is expected to decrease from shear instability of the flux lattice. [S0163-1829(96)00925-3]

I. INTRODUCTION

The current density in most $YBa_2Cu_3O_{7-\delta}$ single crystals and also in melt-textured samples approaches a maximum value j_{max} at a magnetic field B_{max} far above the self-field. This ''fishtail'' or ''peak'' effect (PE) is observed in ac and dc inductive measurements in the geometry magnetic field B parallel to the c axis of the crystal ($B\|c$) and j flowing within the a,b plane (for instance, Ref. 1). Recently the PE was observed also in resistive transport measurements in the same geometry $B\|c$ and $j\|a,b$.[2,3] For $B\|a,b$ however it is claimed in various papers (for instance, Ref. 4) that the PE vanishes. The mechanisms as well as the defect structure responsible for the PE have still not been clarified. Recently pointlike defects resulting in a current which is governed by softening and plastic flow of the flux lattice have been discussed.[5,6] In this case the PE is related to an isotropic defect structure and should be observed also in the geometry $B\|a,b$. This question was one motivation for a careful investigation of the PE in dependence on the angle between magnetic field and crystal orientation, especially in the vicinity of $B\|c$ and $B\|a,b$. Because the PE results either from impurities or in very clean samples from oxygen vacancies[5] and is influenced by twin boundaries,[7,8] the investigation was carried out on four crystals with different defect concentration, different kinds of pointlike defects, and different twin structures. Besides the current along a,b for $B\|c$ also the currents along a,b and along c for the geometry $B\|a,b$ are obtained and discussed.

The second investigated topic is the influence of the twin structure and the CuO planes on the PE and the irreversibility field. For the study of the interference between flux pin-

TABLE I. Characterization of the investigated crystals. Irreversibility fields B_{irr} and currents are given for the geometry $B \| c$.

Crystal	1	2	3	4
R	Y	Y	Tm	Y
T_c (K)	91.2	89.4	88.4	90.1
B_{irr} (T) at 77 K	≈9	4.28	4.01	5.19
j_{max} (A/cm^2)	8.01×10^4	6.72×10^4	4.85×10^4	8.01×10^4
at 77 K, B_{max}	(2.56 T)	(1.19 T)	(1.44 T)	(2.16 T)
Oxygen vacancies	+	−	−	−
Point defects	−	+	+	+
Twins	+	+	(−)	−
Size $a\times b\times c$ (mm^3)	$2.04\times0.69\times0.03$	$1.50\times1.08\times0.125$	$1.27\times1.25\times0.219$	$1.04\times0.97\times0.1$

ning from correlated and pointlike defects the angular dependence of the magnetic moment is measured and compared with the results from untwinned crystals. In addition to the angular dependence the different influence of planar and point defects is also observed in the behavior of the relaxation rate and in the field dependence of the current. Finally, in the third part, lock-in oscillations of the magnetic moment vs field in $B \| a,b$ are observed and discussed.

II. EXPERIMENTAL

The magnetic moment m of an induced shielding current was measured with a vibrating-sample magnetometer (Oxford Instruments). The angle ϕ between the magnetic-field direction and the c axis of the crystals could be varied within a precision of $\pm0.1°$. A Ni foil in the saturated state with about the same size as the sample was used for calibration of the magnetometer. The measured magnetic moment of the Ni foil vs ϕ between 0° and 360° deviates from the expected constant value by about 1% at 7 T. Measurements of the crystals were made as a function of ϕ, B, and temperature T at a constant sweep rate of the magnetic-field $dB/dt=10^{-2}$ T/s. The normalized relaxation rate $S=(d\ln(\Delta m))/(d\ln(dB/dt))$ was obtained from $m(B)$ measured at various dB/dt values. Four $RBa_2Cu_3O_{7-\delta}$ single crystals with different kinds of pointlike defects and twin structures were studied. All samples showed a pronounced PE in the geometry $B \| c$. The midpoint of the transition temperature T_c, the irreversibility field B_{irr}, the maximum current density j_{max} and the field B_{max} at which these currents were observed are given in Table I. The current was determined from the difference of m between increasing and decreasing magnetic field $\Delta m \sim j$ measured with a constant electric field $E \sim dB/dt$ of about 0.1 μV/cm at the sample surface. The irreversibility fields correspond to the same E criteria and to a current of $10^{-2}\times j_{max}$. The T_c values are obtained from zero-field-cooled and field-cooled measurements using a field of 10^{-3} T.

The crystals were grown from CuO-BaO flux in ZrO_2 or Al_2O_3 crucibles by the slow-cooling method.[9] In Table I the dominating defects in the crystals are indicated by ''+'' whereas ''−'' means that this type of defect is of negligible influence. This qualitative information is based on optical and transmission electron microscopy studies and on different methods concerning the determination of the impurity content. The purest crystal 1 had a continuously decreasing j vs B above 70 K. This means no PE for oxygen deficiency $\delta \leqslant 0.01$. The crystal was then subsequently deoxidized which results in different values of δ. Figure 1 shows the corresponding current density vs magnetic field at three different oxidation states. After the final step in an atmosphere of 1 bar oxygen at 460 °C during 150 h, which corresponds to $\delta=0.04$, according to Ref. 10 the crystal exhibited a pronounced PE and was used for the present investigations. The PE in this crystal is therefore related to oxygen vacancies along the CuO chains. In crystals 2, 3, and 4 the PE is present above 70 K for all oxygen contents. The pointlike defects responsible for the occurence of the PE result from impurities. Crystal 2 was doped with about 6% Sr on Ba sites. As determined by inductively coupled plasma-mass spectroscopy analysis the fluxes from which crystals 1 and 2 were grown did not contain more than 300 ppm of metallic impurities in addition to Hf and Zr. All crystals are grown in Y-stabilized ZrO_2 crucibles except crystal 3 which was grown in an Al_2O_3 crucible. This led to an Al-substitution of approximately 1–2 % of the chain Cu site, as estimated from the T_c reduction. The dominating point defects in crystal 4 are not yet identified. Crystals 1 and 2 have an ordinary twin structure; the twin spacing in both crystals observed by TEM is 440 and 190 nm, for crystals 1 and 2, respectively, with a narrower twin-size distribution in crystal 2. The twin lamellas extend along the (110) direction by a few hundred μm in crystal 1 and up to 1 mm in crystal 2. Crystal 3 is nearly twin free in the as-grown state with a monodomain area of roughly 80% of the sample size. Crystal 4 was detwinned by applying a uniaxial pressure of about 10^8 N/m^2 at 400 °C for about 10 min. After this treatment the crystal was investigated by polarized light microscopy and the remaining twinned areas were removed by cutting.

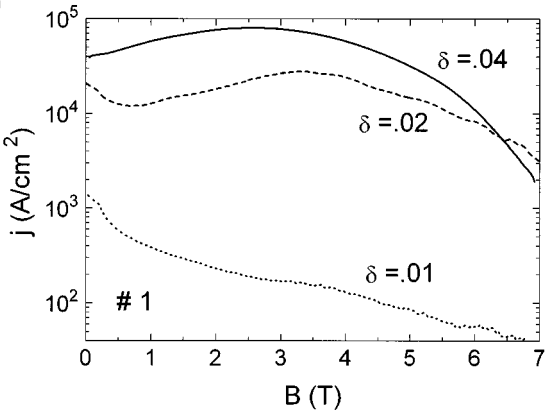

FIG. 1. Current density j vs magnetic field B at 77 K for crystal 1 in 3 different oxidation states.

In summary, the PE results from oxygen vacancies in crystal 1 and from different impurities in crystals 2, 3, and 4. In crystals 1 and 2 the influence of the twin structure is present. Twins are of minor influence in crystal 3 and completely absent in crystal 4. We restrict the discussion to the temperature region around 77 K in order to exclude possible changes of the pinning interaction or influences from defects

becoming effective at lower temperatures.

The sizes given in Table I correspond to the as-grown states of the samples which were close to a rectangular shape. After the measurements, crystals 1, 2, and 3 were cut into a rectangular shape with a high aspect ratio along the a,b plane in order to determine the currents in the geometry $B\|a,b$ from two measurements with the field direction along both sides of the rectangle. The tilting plane of the magnetic-field direction from the c axis was parallel to these crystal sides and has therefore an angle of 45° with the twin boundaries. This means that in the geometry $B\|a,b$ twin boundaries interact with the flux-line lattice approximately like point defects.

III. RESULTS AND DISCUSSION

The angular dependence of the current is one of the most efficient tools to distinguish between different pinning mechanisms.[11] The measurement of the magnetic moment from the shielding current in platelike samples requires us to consider the geometrical influence[12] and the two current contributions. Isotropic uncorrelated disorder produces a current density with a smooth angular dependence connected with the intrinsic anisotropy of the superconductor whereas a very sharp variation is expected from correlated disorder produced by plane and line defects. The scaling approach from Ref. 13 to collective pinning in the single vortex regime allows us to calculate the in-plane current as a function of angle ϕ and anisotropy parameter Γ. For the moment determined by the current in the a,b plane of a thin platelike crystal,[12] this relation reduces to the c-axis component model[14] discussed below. From the scaling approach the current densities along a, b, and along c should have the same field dependence and the ratio $(j\|a,b)/(j\|c)$ should correspond to Γ. The scaling analysis which gives the same relation in the small bundle regime becomes inapplicable in the large bundle regime.

Correlated pinning centers as twin boundaries, CuO planes or columnar tracks result in a very sharp angular dependence of the current. The theory predicts[15,16] that at small tilting angles (about 1° for twins) vortices are locked into the twin boundaries. In this range shielding currents should be independent of ϕ. At angles above, the locking breaks and vortices divide into sections pinned in the bulk and at the twin boundaries. Finally, after exceeding the trapping angle these kink vortices vanish and they become aligned with the magnetic field. The same scenario should work for intrinsic pinning by the CuO planes, only the characteristic angles should be significantly smaller.

In the following we discuss in Sec. III A the angular dependence of the obviously dominating peak effect. Sections III B and III C are related to the influence of the twin structure and the CuO planes, respectively, on the irreversibility field and the current. In the appendix we describe the unexpected behavior of the magnetic moment in the geometry $B\|a,b$ after the crystals were cut.

A. Angular dependence of the peak effect

In Figs. 2(a)–2(d) the hysteresis width $\Delta m(B)$ is plotted for the four crystals at different angles from $\phi=0°$ ($B\|c$) to $\phi=90°$ ($B\|a,b$) at 77 K. The PE has a maximum Δm for

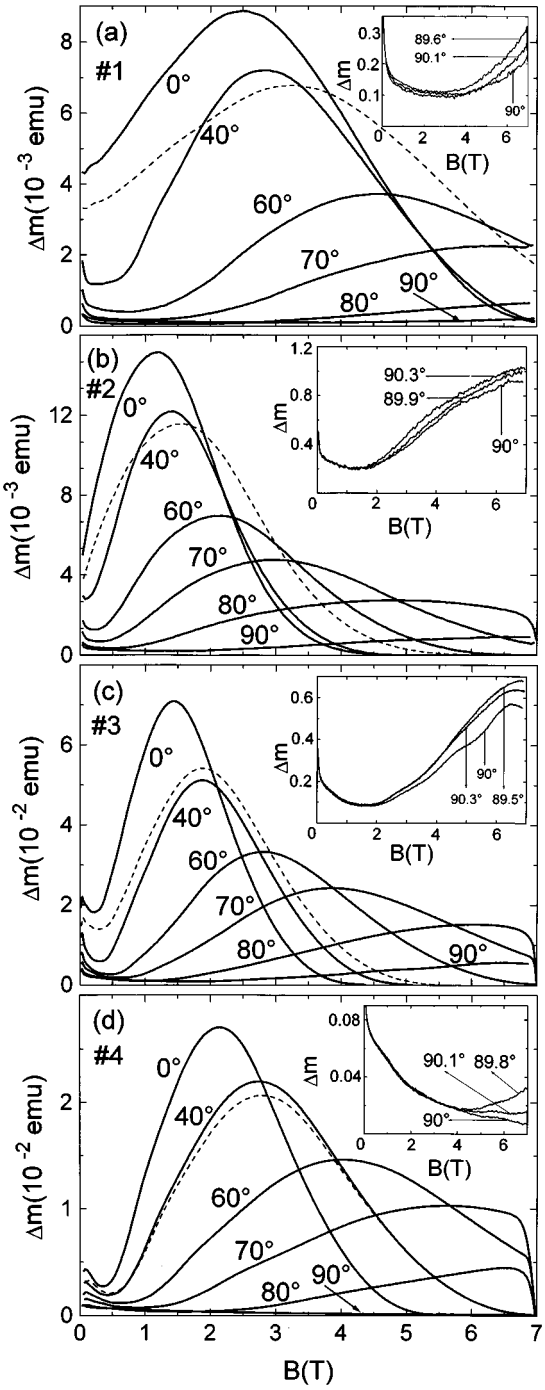

FIG. 2. (a)–(d) Difference of the magnetic moment between increasing and decreasing branch of the magnetization (hysteresis width) Δm vs magnetic field B for the four crystals at 77 K. The angle between B and the c axis of the crystals varied between 0° and 90°. The insets show the angular region very close to 90° which corresponds to $B\|a,b$. The dashed line represents the c-axis component of Δm $(B,\phi=40°)$ calculated from the measurement at 0°.

$B\|c$ which decreases with ϕ mainly due to the decrease of the effective scaling length within which the currents flow (from b to c, see Table I). From the variation of the superconducting parameters as coherence length ξ and London penetration depth λ, an increase of the current density is expected from $B\|c$ to $B\|a,b$ above the current peak. In the measured Δm values this increase, however, is partly sup-

pressed by the geometrical influence. Further, the twin plane structure—being effective planar pinning centers only within the trapping angle at $B\|c$—is also responsible for the anisotropic behavior.

In previous studies of untwinned crystals it was shown that within a large angle region from the c axis the angular dependence of Δm is determined by the c-axis component.[4] In the twinned crystals 1 and 2 the value $\Delta m(B)$ as a function of ϕ does hardly correspond to its component along the c axis. The dashed line represents the c-axis component for $\phi=40°$ calculated from

$$\Delta m(B/\cos\phi,40°)=\Delta m(B,0°)\cos\phi, \qquad (1)$$

where the out-of-plane magnetization is neglected.[14] This c-axis component calculated from the measured moment at $\phi=0°$ is lower in the peak region and larger below and above the peak in comparison to the measured value at 40°. This difference which is caused by twins shall be discussed in more detail in Sec. III B. The influence of the correlated disorder in the flux lattice from twins is therefore reflected in the quite different field dependences of Δm at $\phi=0$ in comparison to Δm at higher angles. As can be seen from the difference between $\Delta m(B,40°)$ and the calculated values from Eq. (1) (dashed line), the correlated disorder influences $\Delta m(B,0°)$ most pronounced in crystal 1, and to a much lesser extent in crystal 2, in spite of similar twin structures and comparable current densities at $B_{\max}$. This means that the pointlike defects from Sr doping in crystal 2 produce a stronger pinning than the oxygen vacancies in crystal 1. This may be related to the significantly larger concentration of point defects in sample 2.

The untwinned crystals 3 and 4 show $\Delta m(B,\phi)$ values which are very close to their corresponding c-axis component. The field dependence of Δm at $\phi=0$ is very similar to those at higher angles in contrast to crystals 1 and 2. Generally the field dependence of Δm at angles above the trapping value from the twins becomes very similar for all four crystals. It shows then a good scaling behavior if B is normalized by $B_{\rm irr}$ and Δm by its maximum value. This supports pointlike defects as being the responsible defect structure for the PE.

From the measurements of $\Delta m(B)$ at 40° where twins are of minor influence Δm and $B_{\max}$ for higher angles are calculated using the modified equation (1) and $B_{\max}(\phi)=B_{\max}(40°)(\cos 40°)/(\cos\phi)$. The measured $\Delta m(\phi)$ values become larger than the calculated ones, whereas the measured $B_{\max}(\phi)$ are below their corresponding calculated values. From the out-of-plane magnetization and the anisotropy these expected deviations of Δm and $B_{\max}$ between experimental and c-axis components increase with angle, especially the PE does not vanish for $B\|a,b$. The insets in Fig. 2 demonstrate the presence of the PE at $B\|a,b$ and in the region very close to it. The appearance of the PE in this geometry, which was checked by 0.1° steps of the angle, cannot be produced by misalignment. At $\phi=90°$ and at any angle above or below, Δm increases with B.

The measurement of crystal 4 at $\phi=90°$ [inset of Fig. 2(d)] shows a decreasing Δm value with field. This absence of the $\Delta m(B)$ peak up to 7 T within an angle window of about 0.2° can hardly be related to a smooth angular dependence of the pinning interaction from pointlike defects but to the interaction with the CuO planes. This effect is expected to become most pronounced in twinfree and very pure crystals. The not observed maximum in Δm may be caused by a very sharp peak of $B_{\rm irr}$ vs ϕ, shifting the field at which Δm approaches its minimum above 7 T at 77 K. In order to investigate this possibility we measured Δm at $B\|a,b$ from 77 to 82 K (Fig. 3). Unfortunately the magnetic moment in the interesting higher field region decreases rapidly with temperature reaching the experimental noise level at about 80 K. The measurement at 79 K shows only a very shallow minimum (inset of Fig. 3) which points to the presence of the PE. Another possibility for the absence of this phenomenon at precisely $90\pm0.1°$ may be related to the different currents from which Δm (90°) results. The current along the c axis, $j\|c$, and along the a,b plane, $j\|a,b$, contributes to Δm:

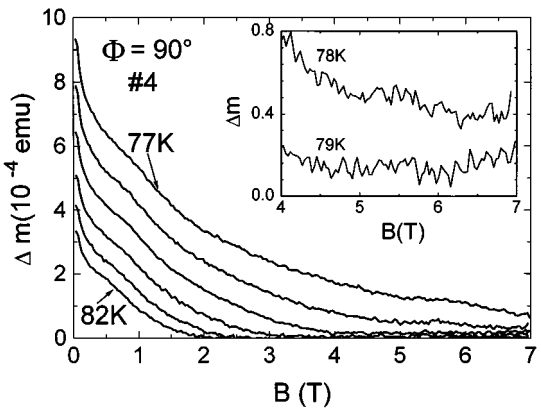

FIG. 3. Hysteresis width Δm vs magnetic field B at different temperatures from 77 up to 82 K in 1 K steps. The inset shows $\Delta m(B)$ in the higher field region.

$$\Delta m/V=(j\|a,b)c/2\{1-[(j\|a,b)c]/[(j\|c)3a]\}. \qquad (2)$$

V is the volume and c and a represent the thickness of the crystal along the c axis and along the side perpendicular to it. The extended Bean model[17,18] assumes isotropy of the current flow within the a,b plane. Equation (2) requires further that $(j\|c)a$ is smaller than $(j\|a,b)c$, a condition which is satisfied in the crystals. The current $j\|c$ may decrease either from low pinning or from the impeding current flow perpendicular to the CuO planes or from easy guided motion of flux lines parallel to the CuO planes. In the last case no PE is expected for $j\|c$ if channeling dominates. Further, the current along the a,b plane may increase due to intrinsic pinning of the flux lines within the CuO planes. This also depresses the pinning from pointlike defects. The observed sharp angular dependence of Δm excludes probably a low current flow parallel to the c axis as a possible origin for the absence of the PE. The other possibilities, channeling and intrinsic pinning, as well as the possible lock-in transition of flux lines shall be further discussed in Sec. III C.

As mentioned above, the shielding current in $B\|a,b$ is flowing along the a,b and along the c axis of the crystal and therefore the measured moment results from these two contributions. The most direct way to eliminate the geometrical influence, to check which current dominates, and to prove the PE in the geometry $B\|a,b$ is to discriminate between the two current components. For this reason crystals 1, 2, and 3

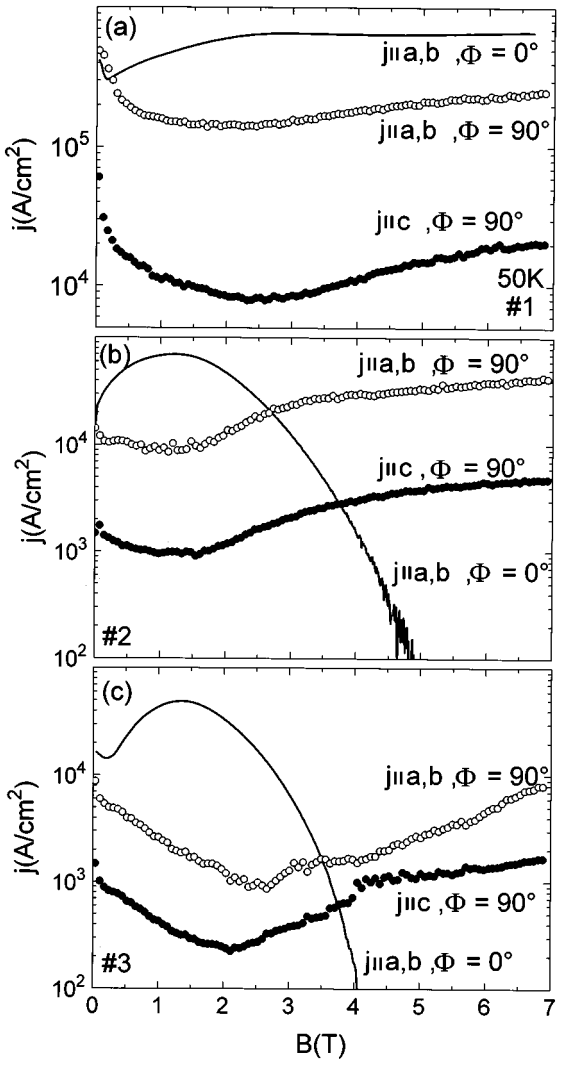

FIG. 4. (a)–(c) Current density j vs magnetic field B for crystal 1 at 50 K and for crystals 2 and 3 (b,c) at 77 K. The bold line corresponds to j flowing along the a,b plane with B parallel to the c axis of the crystal. Open circles represent j parallel to the a,b plane and B perpendicular to the c axis and closed circles j parallel and B perpendicular to the c axis.

were cut along the a,b plane in a rectangular shape with a high aspect ratio and measured in $B\|a,b$ twice: with B parallel to the larger and to the smaller side, respectively. The current ($j\|a,b$) and the current along the c axis $j\|c$ for $B\|a,b$ were calculated using Eq. (2). In Figs. 4(a)–4(c) the results are shown together with the current $j\|a,b$ for the geometry $B\|c$. As expected from Fig. 2 both values $j\|a,b$ and $j\|c$ for $\phi=90°$ show the PE in the three crystals. The different ratios of the currents $(j\|a,b)/(j\|c)$ which vary between about 3 in crystal 3 and 15 in crystal 1 reflect a larger anisotropy in the purer crystal 1 assuming a similar anisotropic interaction from pointlike defects in the crystals or it reflects the influence of the oxygen deficiency on the anisotropy in crystal 1. The much lower current density flowing along c is caused by the anisotropy of the elementary pinning forces and elastic moduli of the flux lattice, by the direction of the Lorentz-force acting parallel to the CuO planes, and by the impeded or imperfect current flow along the c axis. The presence of the PE in all geometries supports pointlike defects as being the responsible defect structure for this phenomenon and it shows that the PE in these crystals dominates in comparison to the other competing mechanisms in this geometry. The plateaulike field dependence of the current for $B\|c$ in crystal 1 at 50 K [Fig. 4(a)] results from easy flux channeling along the twin planes as discussed in Refs. 19 and 20.

B. Irreversible behavior in the vicinity of $B\|c$

In this part the influence of the twin structure and its interference with pointlike defects is investigated. In the vicinity of $B\|c$ twins determine the irreversibility field, the current (as already shown in Sec. III A) and its relaxation behavior. The theoretical models in context to this interference and to the issue of this section are reviewed and extensively discussed by Blatter *et al.*[16]

In clean untwinned crystals a first-order phase transition is favored to be the origin of the crossover from vortex solid to vortex liquid.[21] This melting which occurs at 77 K at about 8 T is influenced by vortex pinning. Disorder from pointlike defects smears out the melting transition and transforms it into a second-order vortex-liquid–vortex-glass crossover.[22] Both the melting and the vortex-glass transition fields are expected to have a minimum at $\phi=0°$ and to increase from $B\|c$ towards $B\|a,b$ at $\phi=90°$. The measured irreversibility field, which is criteria dependent, is close to this transition point.[23] The criteria we used for the determination of $B_{\rm irr}$ corresponds roughly to an exponent of $n\approx 2$ if the $E(j)$ characteristics is approximated by a power law $E\sim j^n$. This means that $B_{\rm irr}$ is slightly above the theoretical transitions which are related to somewhat steeper $E(j)$ curves.

Correlated defects like amorphous columns from heavy ion irradiation or twins should modify and shift the vortex-glass transition into the vortex liquid towards higher fields. Theories predict a Bose glass transition[24,25] or a two-dimensional melting[16] with a cusplike dependence of $B_{\rm irr}(\phi)$ at $B\|c$. Such a sharp rise of the irreversibility line at $\phi=0°$ is observed in the twinned crystals 1 and 2 as shown in Figs. 5(a) and 5(b). A smooth interpolation of $B_{\rm irr}(\phi)$ to $\phi=0°$ using Eq. (3) results in a trapping angle of about 15° below which vortices interact with the twin planes. The relative increase of $B_{\rm irr}$ at $\phi=0°$ from twins with respect to $B_{\rm irr}$ from pointlike defects is obtained by a smooth interpolation from outside the trapping angles of $\pm 15°$ to $\phi=0°$. The value is about 30% in crystal 1 and 15% in crystal 2 with a more dominating pointlike defect structure. Even crystal 3 shows a shallow maximum with an increase of about 5% [Fig. 5(c)] in comparison to the minima of $B_{\rm irr}$ on both sides of $B\|c$. This somewhat unexpected effect may be caused by the small number of remaining twins observed by optical polarized light microscopy. Only the twin-free crystal 4 shows the monotonous decrease of $B_{\rm irr}(\phi)$ towards $B\|c$ expected from a pointlike defect structure in an anisotropic homogeneous superconductor [Fig. 5(d)]. However, in the original state after detwinning where a small number of twins were still present, this crystal also showed a $B_{\rm irr}$ peak. From these observations in Figs. 5(a)–5(d) the transition at $\phi=0°$ into the vortex liquid seems to be determined by twins in the crystals 1, 2, and 3. This rejects a vortex-glass transition as predicted for pointlike disorder. Resistive measurements in samples 1

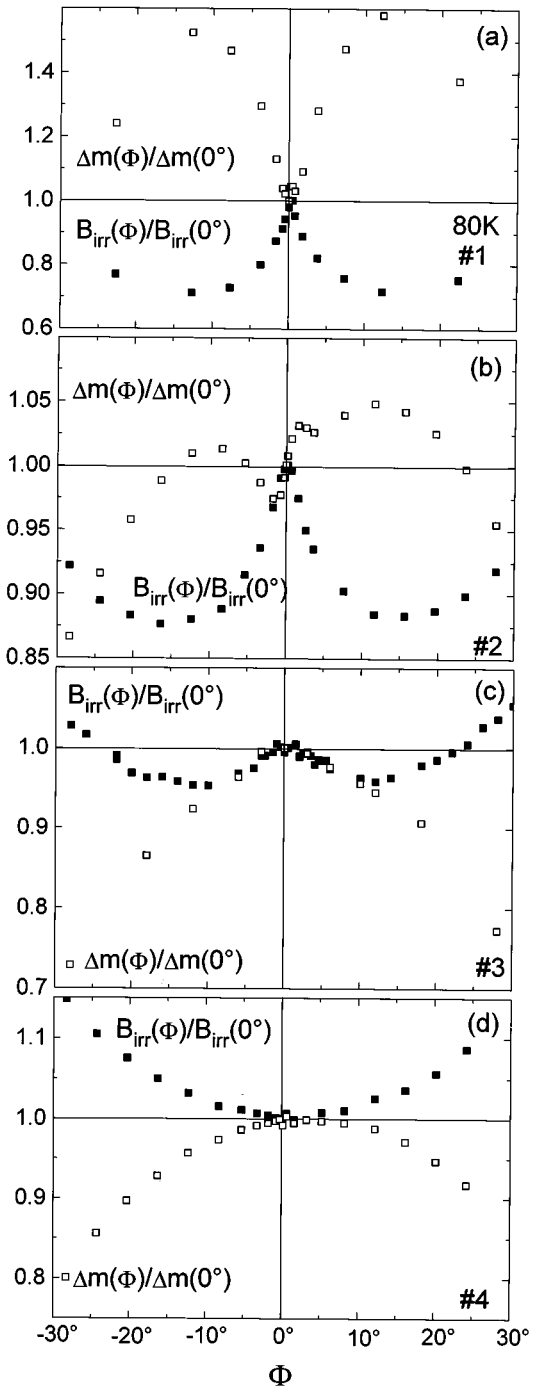

FIG. 5. (a)–(d) The angular dependence of the normalized hysteresis width $\Delta m(\phi)/\Delta m(0°)$ taken at the peak position (open squares). Measurements are made at 80 K for crystal 1 (a) and at 77 K for the other crystals. The filled squares represent the corresponding values of the normalized irreversibility fields $B_{\rm irr}$.

and 2 indeed did not reveal $E(j)$ characteristics which are expected for a vortex-liquid–vortex-glass transition.[26] An estimation of $B_{\rm irr}$ determined by pointlike defects from the extrapolation of $B_{\rm irr}(\phi)$ to $\phi=0°$, results for the same reduced temperature $T/T_c=0.855$ (77 K for crystal 4) in 5.55, 4.59, 4.8, and 5.19 T for crystals 1, 2, 3, and 4, respectively. The order of decreasing purity of the studied crystals 1-4-3-2 is in correspondence with the behavior of $B_{\rm irr}$ and indicates that the transition field decreases with increasing impurity content.

For an isotropic pinning structure one expects a maximum current at $B\|a,b$ and a decrease towards $B\|c$ resulting from the monotonous change of superconducting parameters such as λ, ξ, and B_{c2}. The corresponding behavior of Δm is depressed by the highly platelike structure of the crystals. Turning the crystal from $\phi=0°$ at $B\|c$ to larger angles reduces the magnetic moment proportional to $\cos\phi$ neglecting the angular dependence of the superconducting properties. Such a simple behavior is observed in the twin-free crystal 4 where Δm vs ϕ passes a broad maximum at $\phi=0°$ for all magnetic fields except close to $B_{\rm irr}$. As an example Fig. 5(d) shows $\Delta m(\phi)$ reduced by $\Delta m(0°)$ where both values are taken at $B_{\rm max}$. The small asymmetry of $\Delta m(\phi)$ and $B_{\rm irr}(\phi)$ with respect to $\phi=0°$ in Fig. 5(d) may be caused by an always present nonideal rotation of the sample around to its symmetry axis.[27]

In crystal 3 the small number of twins which slightly increases $B_{\rm irr}$ does not influence the current at lower fields. Therefore $\Delta m(\phi)$ at $B_{\rm max}$ shows also a broad maximum at $B\|c$ from isotropic pointlike defects and from the angular variation of the geometry of the crystal with respect to the field direction [Fig. 5(c)]. Only at fields closer to $B_{\rm irr}$ $\Delta m(\phi)$ reflects the more pronounced increase at $\phi=0°$ from the transition governed by twins. If the twin structure is fully developed and dominates in comparison to other pinning sites the current shows in the whole field region a very sharp, cusplike increase at $B\|c$ caused by the interaction between flux lines and twin planes. If the field is tilted away from $B\|c$ the length at which vortices are strongly pinned by the twin walls decreases and finally shrinks to zero at the trapping angle. In the presence of pointlike defects this behavior is still observed as long as the corresponding pinning is not very strong in comparison to the interaction between twins and vortices. This is the case in crystals without a PE, in less pure crystals at fields very close to $B_{\rm irr}$, or at high temperatures where twins always dominate. But in crystals with a PE another phenomenon is additionally observed in the presence of twins. Vortices are pinned by pointlike defects between the twin walls and by the twin walls itself. If the Lorentz force or a component of it is directed parallel to the twin walls the force of the vortex lattice against shearing may determine the current. This requires that the interaction of vortices with the high density of pointlike defects exceeds the longitudinal twin wall interaction. In this case plastic deformation occurs if the shear force of the vortex lattice becomes smaller than the pinning force from pointlike defects. Then flux channels along the twin walls under the influence of the longitudinal component of the Lorentz force. This channeling process which was discussed first in Ref. 19 approaches a maximum at $B\|c$, which corresponds to a minimum in $\Delta m\sim j$. This interference between correlated and pointlike disorder is observed in crystals 1 and 2 [Figs. 5(a) and 5(b)] in an angular region which coincides approximately with the trapping angle. The decrease of Δm ($\phi=0°$) produced by the flux channeling in crystal 1 is much larger than in crystal 2. Taking into account the similar twin spacing of both crystals this difference results partly from the

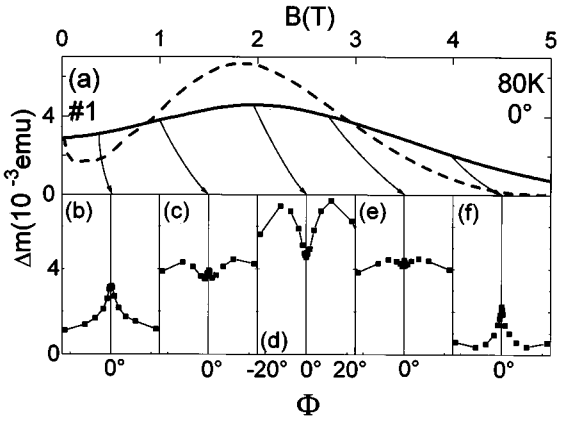

FIG. 6. (a)–(f) Hysteresis width Δm vs magnetic field B at $B\|c(\phi=0°)$, bold line, and calculated Δm from the c-axis component of the measured value at $\phi=40°$, dashed line (a). (b)–(f) show the angular dependences of Δm at different B values indicated by the arrows.

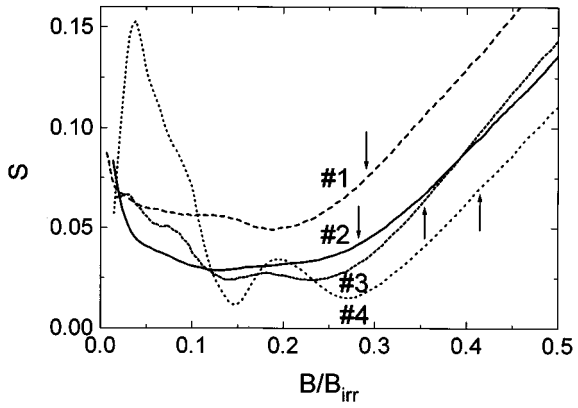

FIG. 7. Normalized relaxation rate S vs magnetic field B normalized by the irreversibility field $B_{\rm irr}$. The arrows indicate the reduced fields at which the current approach the maximum. The measurements are made at 77 K in the geometry B parallel to the c axis of the crystals.

larger current caused by pointlike defects at $B\|c$ in crystal 1 than in crystal 2. Further, possible reasons are the length of the (110) twin walls till they are interrupted by (110) walls oriented perpendicular, the degree of planarity of the twin walls, the possible accumulation of defects in the twin walls, and the orientation of the twin domains with respect to the Lorentz force. These properties result in different ratios between transverse and longitudinal pinning forces of the twin walls in both crystals. The asymmetry of $\Delta m(\phi)$ with respect to $\phi=0°$ is larger in twinned samples and changes after the crystals are cut.

The channeling behavior was found in the temperature region around 50 K,[19,20] where it is correlated with a plateaulike field dependence of the current [Fig. 4(a)]. In the present investigation it is probably also observed at higher temperatures at which Δm $(B,\phi=0)$ does not show such an anomaly. But a comparison of Δm between $\phi=0°$ and its expected value from above the trapping angle reveals a distinct depression of Δm at $B\|c$ just in the peak region where the channeling becomes pronounced. Figure 6(a) shows the measured Δm vs B of crystal 1, the dashed line corresponds to the calculated Δm value for 0° from the measured one at 40°, outside the trapping angle. In Figs. 6(b)–6(f) the angular dependences of Δm between $-20°$ and 20° at different magnetic fields are plotted as indicated by the arrows. The above discussed channeling of vortices is related to the region around $B_{\rm max}$ where $\Delta m(B)$ from pointlike defects is depressed. An alternative explanation for the depression of Δm is an enhanced effective tilt modulus which prevents softening or synchronization of the flux lattice[3] from which the PE may originate. At fields below and above the peak region [Figs. 6(b) and 6(f)] pinning from the twin structure increases Δm as reflected by a sharper maximum and a larger Δm at $\phi=0$ similar to that expected from the comparison between measured and calculated moment [Fig. 6(a)]. In the field region in between [Figs. 6(c) and 6(e)] the transition of the enhancement from pinning to the depression from channeling or stiffer tilt modulus is observed. This demonstrates that the influence of twins for $B\|c$ is important in the whole field region. They influence the field dependence of the current even if their interaction with the vortices does not dominate, for instance in comparison with pointlike defects which cause the PE.

Strong pinning interaction from the transverse and channeling from the longitudinal component of the Lorentz force at twin walls both induce plastic deformation of the flux lattice in the presence of probably elastic distortion from the pointlike defects. This is in full agreement with observations from ac flux-profile measurements in twinned $YBa_2Cu_3O_{7-\delta}$ single crystals with a PE.[6] According to these investigations the reversible flux motion within the Campbell penetration depth is superimposed by irreversible flux movement which points to local plastic shear of vortices.

From the considerable influence of the twin structure on the pinning from pointlike defects a similar influence on the relaxation behavior may be expected. Figure 7 shows the normalized relaxation rate S at 77 K obtained from Δm $(B,\phi=0°)$ measured with various sweep rates. The field is normalized by $B_{\rm irr}$ and the arrows indicate the $B_{\rm max}$ values. There are characteristic differences in $S(B)$ between the twinned crystals 1 and 2 and the twin-free samples 3 and 4. Crystals 1 and 2 show the well-known behavior of S with a shallow minimum. The field dependence of S is very similar in both crystals but crystal 1 with the much more pronounced channeling reveals higher S values. At higher temperatures the twin-free crystals 3 and 4 show a double minimum structure and lower relaxation rates. These characteristic $S(B)$ features which are more developed in crystal 4 are different from the behavior of the twinned crystals in the field region up to 0.3 $B/B_{\rm irr}$. The sharp maximum of S at low fields (crystal 4 in Fig. 7) coincides with the penetration field at which vortices with the opposite direction of the B field reach first the center of the sample. Then at larger fields two minima in S occur which are accompanied by only one maxima in Δm situated at the much larger field $B_{\rm max}$. Obviously at higher temperatures there is no correlation between maxima in Δm and minima in S as seen at 50 K.[20] The influence of the twin structure should about vanish above the trapping angle as for $\Delta m(B)$ if the field direction is tilted away from the c axis. Figures 8(a) and 8(b) show the corresponding measurements as an example for crystals 2 and 4 at

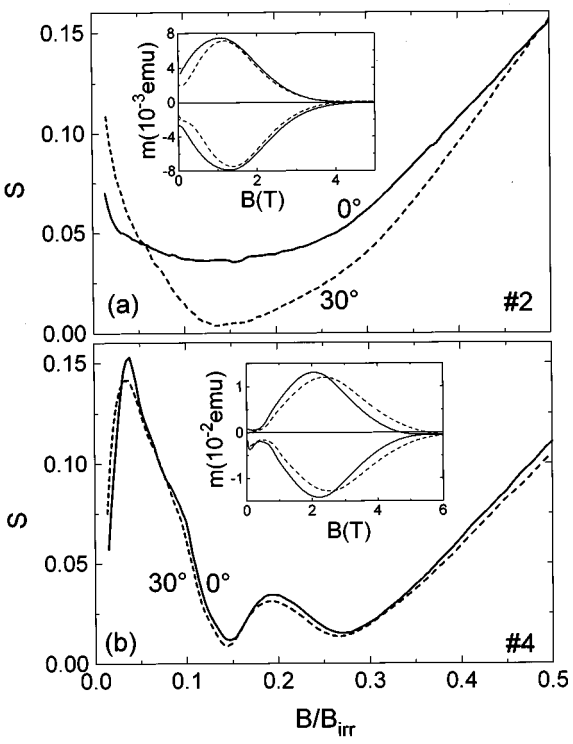

FIG. 8. (a) and (b) Normalized relaxation rate S vs magnetic field B normalized by the irreversibility field B_{irr}. The measurements are made at 77 K in the geometry B parallel to the c axis of the crystal (bold line, 0°) and at an angle of 30° between B and the c axis (dashed line). The insets show the corresponding magnetization vs B.

0° and 30° where the irreversibility fields are not much different. Whereas the twinned crystal 2 reveals remarkable changes of $S(B)$ between 0° and 30° the detwinned sample 4 shows a very similar behavior for the two angles. The S value of crystal 2 at 30° in the field region of its minimum decreases considerably and the field dependence becomes more comparable to the twin-free samples. This comparison clearly demonstrates that the relaxation is also sensitively influenced by the twin structure.

C. Irreversible behavior in the vicinity of $B\|a,b$

First we discuss the angular dependence of the irreversibility field. Only at higher temperatures B_{irr} could be measured also in the geometry $B\|a,b$. Figure 9 shows B_{irr} vs ϕ at 86 K for crystal 2. A change of the voltage criteria by one order of magnitude results in a shift of $B_{\mathrm{irr}}(0)$ by about 10%. This demonstrates that the used criteria for measuring B_{irr} is of minor influence on the result. The value $B_{\mathrm{irr}}(\phi)$ shows a plateaulike behavior from $\phi=0°$ up to about 40° and increases sharply above. The dashed line in Fig. 9 corresponds to the equation

$$B_{\mathrm{irr}}(\phi)=B_{\mathrm{irr}}(0)(\cos^2\phi+\Gamma^{-2}\sin^2\phi)^{-1/2} \qquad (3)$$

based on a scaling approach to an anisotropic homogeneous superconductor where Γ represents the anisotropy parameter.[16] The ratio $B_{\mathrm{irr}}(90°)/B_{\mathrm{irr}}(0°)$ of about 6 is within the reported values. A similar measurement of $B_{\mathrm{irr}}(\phi)$ at higher temperatures was not possible in crystals 1, 3, and 4

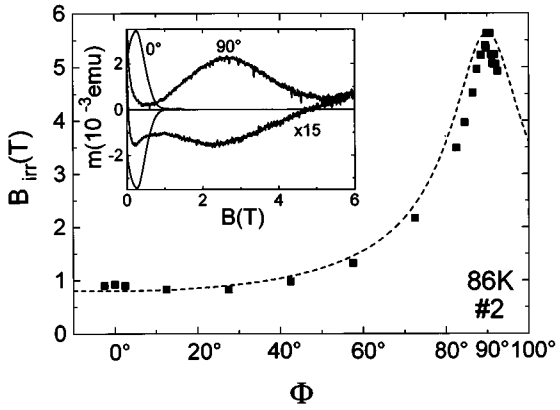

FIG. 9. Irreversibility field B_{irr} vs angle ϕ from $B\|c(\phi=0°)$ to $B\|a,b(\phi=90°)$. The dashed line is the calculated value for an anisotropic homogeneous superconductor with an anisotropy factor of 7. The inset shows the magnetization for $\phi=0°$ and $\phi=90°$.

for different reasons. In crystals 1 and 4 the irreversible magnetic moment at $B\|a,b$ decreases with increasing temperature much faster than in crystals 2 and 3. At 5 T Δm becomes comparable to the experimental noise level above 85 and 80 K in crystals 1 and 4, respectively. For this reason measurements based on the ordinary criteria for determining B_{irr} result in an unphysical decrease of $B_{\mathrm{irr}}(\phi)$ for ϕ approaching 90°. The problem in crystal 3 is the large paramagnetic moment from Tm which dominates above 83 K in comparison to the irreversible superconducting contribution Δm and prevents therefore a precise determination of B_{irr}.

From these measurements at higher temperatures where B_{max} (90°) becomes smaller than 7 T and could be measured, we can estimate the misalignment which would be required for a possible observation of the PE from the c-axis component. For instance, from the ratios $\Delta m(0°)/\Delta m(90°)\approx 30$ (inset of Fig. 9) and $B_{\mathrm{irr}}(0°)/B_{\mathrm{irr}}(90°)\approx 10$ (Fig. 9) one obtains misalignment angles of 2° and 6°, respectively. These values are much larger than the experimental misalignment and internal mosaic spread and demonstrates that the appearance of the PE in $B\|a,b$ cannot be explained by a misalignment.

The interpretation of the pinning behavior in $B\|a,b$ from the measured Δm values is more difficult than for $B\|c$ because the two current components $j\|c$ and $j\|a,b$ contribute to Δm. As in Sec. III A we neglect the possibility of flux-lattice instabilities if the current changes from the a,b to the c direction[28] and discuss Δm in the vicinity of some degrees around $B\|a,b$ within the frame of the extended Bean model. From an isotropic defect structure, such as statistically distributed pointlike defects, one expects for both current densities from the angular variation of B_{c2}, λ, and ξ a smooth maximum at $B\|a,b$. From the geometrical effect of the platelike crystals the corresponding behavior of Δm is depressed as discussed above and a smooth minimum of Δm at $B\|a,b$ may dominate. In contrast to this, the angular dependence of Δm is quite different but similar for all four crystals. As an example Figs. 10(a)–10(e) show $\Delta m(B)$ and the angular dependences between 88° and 92° at 4 different magnetic fields indicated by the arrows. In the lower field region [Figs. 10(b) and 10(c)] Δm passes a smooth maximum in an angular window of about $\pm 1°$. At higher fields the angular depen-

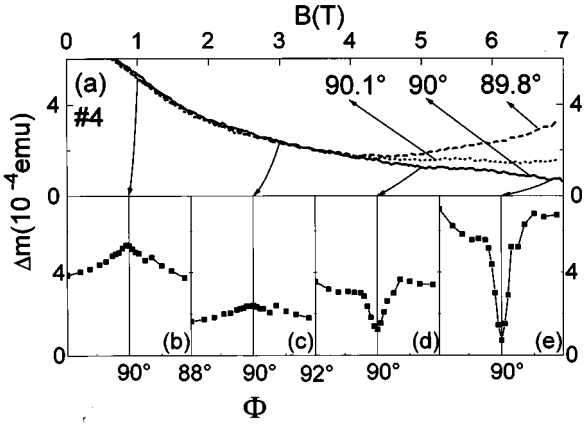

FIG. 10. (a)–(e) Hysteresis width Δm vs magnetic field B at 77 K and different angles between B and the c axis of the crystals in the vicinity of the a,b plane (90° corresponds to $B\|a,b$) (a). (b)–(e) show the angular dependences of Δm at different B values indicated by the arrows.

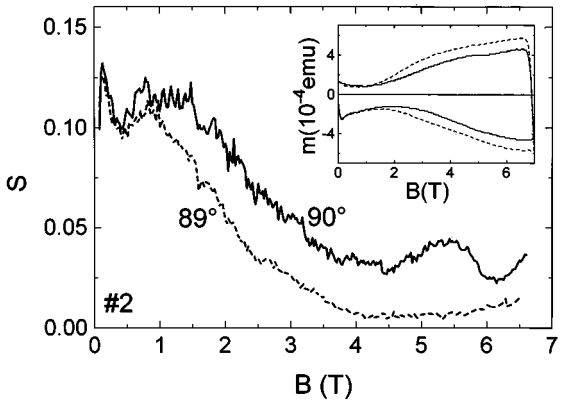

FIG. 12. Normalized relaxation rates S vs magnetic field B measured at 77 K at angles ϕ of 90° and 89° between B and the c axis of the crystal, the inset shows the corresponding magnetization curves.

dence becomes much more pronounced [Figs. 10(d) and 10(e)] and Δm decreases sharply approaching a minimum in an angular window of $\pm 0.2°$. According to Eq. (2) Δm depends on the current contributions from $j\|a,b$ and $j\|c$. A maximum in $\Delta m(\phi)$ at 90° is expected for $j\|a,b$ from intrinsic pinning[29] of the vortices between CuO planes. The trapping angle of approximately 1° [Figs. 10(b) and 10(d)] is in good agreement with the theory.[16] For the Lorentz force parallel to the CuO layers the shear modulus of the flux lattice is predicted to approach an instability at $B\|a,b$.[30,31] This may result in easy motion or channeling of vortices along the CuO planes and decreases the current along the c axis. From both, intrinsic pinning and shear instability, the ratio $(j\|a,b)/(j\|c)$ of Eq. (2) is expected to increase considerably for ϕ towards 90°. We propose this as one possibility for the appearance of the dip in Δm. If the dip becomes very pronounced as in crystal 4, $j\|c$ which is determined by the channeling dominates Δm and the PE vanishes.

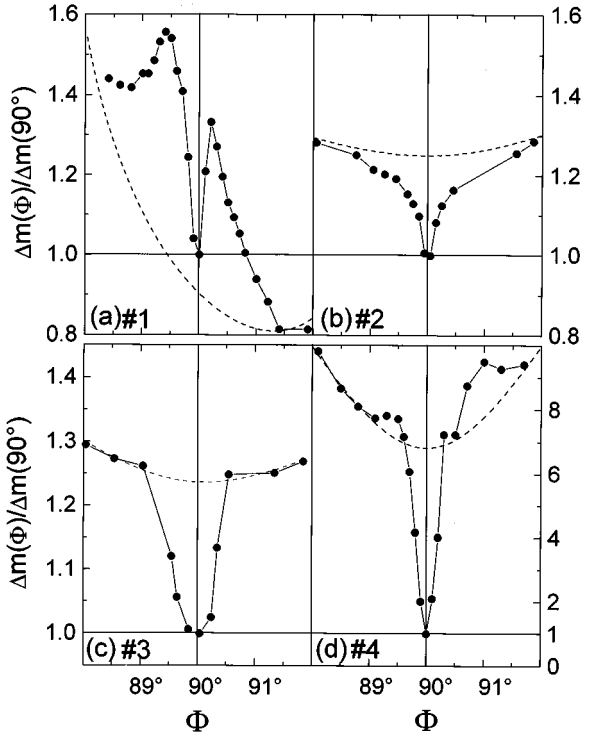

FIG. 11. (a)–(d) Hysteresis width Δm vs angle ϕ divided by Δm at $\phi=90°$ ($B\|a,b$) at 77 K and $B=6.7$ T. The dashed lines are explained in the text.

The decrease of $\Delta m(\phi)$ at higher fields is less severe in the other crystals as shown in Figs. 11(a)–11(d). Common to all samples besides this dip there are also the maximum of $\Delta m(\phi)$ at lower fields and the transformation between the two features in a relatively small field interval. For instance, in crystal 4 the transformation at 77 K occurs between 3.9 and 4.1 T [Fig. 10(a)]. For the explanation of the field dependence of both observations as well as for a quantitative description further investigations are necessary. The characteristic trapping angle for intrinsic pinning may be somewhat larger than the angle below which channeling starts. This explains the increase of $\Delta m(\phi)$ in crystals 1 and 4 before the dip is dominating [Figs. 11(a) and 11(d)]. The dashed lines in Figs. 11(a)–11(d) are guidelines for the eye representing a rough extrapolation of Δm without the interaction from the CuO planes. The large asymmetry of $\Delta m(\phi)$ of crystal 1—far beyond the experimental error—is not yet understood. Both mechanisms intrinsic pinning and channeling are expected to become more pronounced in purer samples, i.e., lower background current at $B\|a,b$. This correlation between purity and relative depth of the dip at $B\|a,b$ is qualitatively observed.

Relaxation measurements in the geometry $B\|a,b$ suffer from the same problems as mentioned above. Figure 12 shows the normalized relaxation rate S vs B obtained from Δm measured with different sweep rates at 90° and 89°. The lower current along the c axis for $B\|a,b$ is in qualitative agreement with higher absolute R and normalized S values at 90° in comparison to 89°. The field dependence of S at 89°, outside the Δm dip, shows a shallow minimum which points to a similar correlation between $S(B)$ and $\Delta m(B)$ as in $B\|c$ for the PE. Larger S values at 90° than at 89° originate probably from the guided motion of flux lines along the a,b planes. This is in full agreement with the behavior near the c

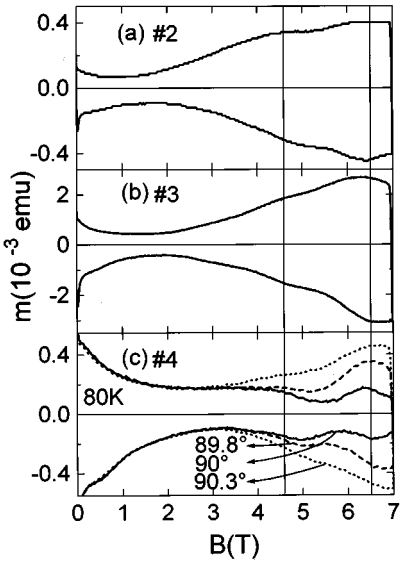

FIG. 13. (a)–(c) Magnetization curves $m(B)$ at 77 K in the geometry $B\|a,b$ (90°) (a,b) and at 80 K at different angles (c).

axis in twinned crystals where larger S values at 0° than at 30° are presumably produced by flux channeling in twin planes.

At $\phi=90°$ $S(B)$ shows an oscillation at higher fields, a maximum at 5.4 T and minima at 4.5 and 6.2 T. The same structure as in $S(B)$ is also observed in $\Delta m(B)$ within an angular region of $90°\pm0.2°$ in all crystals except crystal 1. These lock-in oscillations, found by Oussena *et al.*[32] occur within the dip of the Δm and reflect possibly the increased probability of the channeling process in the case of commensurate vortex-vortex and interlayer CuO distances. These results disprove the possibility of cracks being the reason of the $m(\phi)$ dip near the a,b plane. Figures 13(a)–13(c) show that the oscillations of the magnetic moment become more pronounced from the twinned crystal 2 to the detwinned crystal 4, whereas no such feature was observed in crystal 1. The channeling determines $j\|c$ whereas intrinsic pinning and the related oscillations correspond to $j\|a,b$. The PE which is present in crystals 2 and 3 in $B\|a,b$ does not prevent lock-in oscillations but makes it less pronounced as expected for any other pinning interacting as for instance from twins. The maxima of $\Delta m(B)$ are at 4.6 and 6.5 T indicated by the vertical thin lines in Fig. 13. At these fields intrinsic pinning results in a matching between the flux-line spacing and the CuO layer distance. The related period $\Delta B^{-1/2}$ between these two oscillations corresponds to 0.074 $T^{-1/2}$ which is in agreement with the values given in Ref. 32 for the a and b axes. The maxima in m of Fig. 13 correspond quite well to the minima in S of Fig. 12, which supports the expected lower relaxation in the case where the Lorentz force is directed perpendicular to the CuO planes and the flux lattice accomplishes matching conditions.

IV. CONCLUSION

The interference between correlated disorder in the flux lattice (from twins and CuO layers near $B\|c$ and $B\|a,b$, respectively) and pointlike disorder was investigated in $R\mathrm{Ba_2Cu_3O_{7-\delta}}$ (R=Y, Tm) single crystals. The pointlike disorder originating from oxygen vacancies, impurities or doping is responsible for the peak in the current density vs field resulting in high current values (8×10^4 A/cm^2 at 2.5 T, 77 K). The four studied crystals are different with respect to the randomly distributed pointlike defect and the twin structure. Magnetization loops were measured at fields up to 7 T as a function of angle between the c axis of the crystals and the applied magnetic field. The twin walls form an angle of about 45° with the sides of the rectangular shaped crystal and are parallel to the field direction only at $B\|c$. The tilting plane of the magnetic field was parallel to the side of the crystals. Such orientation keeps twin lamellas equivalent during rotation.

The peak or fishtail effect appears in the two twinned crystals, in the naturally untwinned, and in the detwinned crystal. The phenomenon was present at all angles from $B\|c$ to $B\|a,b$. Using the anisotropic Bean model it is further demonstrated that the peak effect at $B\|a,b$ is observed for both currents $j\|a,b$ and $j\|c$. Such an insensitivity to the presence of twins and to their orientation supports the connection of the peak effect with an isotropic pointlike defect structure and rejects twin boundaries as a possible origin for the peak in these crystals.

The influence of the twin structure on the peak behavior in the vicinity of $B\|c$ is studied by the angular-dependent measurements of the magnetic moment and from comparison with the twin-free crystals. In the twin-free crystals the magnetic moment vs angle passes a smooth maximum at $B\|c$ as expected from the geometrical shape of the crystals. Contrary to this, the twinned crystals show a cusplike increase of the current at $B\|c$ below and above the peak due to pinning of vortices at the twin walls. But in the field region of the peak a pronounced dip at $B\|c$ is observed. This decrease may be explained either by channeling of vortices along twin walls or by an enhanced effective tilt modulus of the flux lattice both depressing the high current peak mechanism. These observations are in full agreement with different $j(B)$ dependences between measurements at $B\|c$ and at angles above the trapping value of about 15°. The relaxation rate in the peak region of the current is lower in twin-free and in twinned crystals outside the trapping angle. This is in accordance with flux channeling along twin walls and this mechanism is favored also for the depression of the current in the peak region in contrast to an enhanced stiffness of the tilt modulus. The twin structure is also responsible for the larger irreversibility field at $B\|c$ (9 T at 77 K) in comparison to twin-free crystals (5 T at 77 K) with the same current density at the peak.

The influence of the CuO layers on the current in the vicinity of $B\|a,b$ is qualitatively the same in twinned and twin-free crystals. An increase of $j\|a,b$ at $B\|a,b$, from intrinsic pinning is observed within a trapping angle of about 1°. This pinning of vortices between CuO layers is further proved by oscillations of the magnetic moment synchronous with the relaxation rate. Maxima of the moment and minima of the relaxation occur at the same temperature-independent fields and follow the matching condition between CuO layer spacing and flux lattice spacing. In the vicinity of the a,b plane the sharp decrease of Δm at higher magnetic fields originates from the current along the c axis decreasing

strongly at $B\|a,b$, possibly due to shear instability of the flux lattice. This mechanism dominates at higher fields contrary to the angular-dependent increase from intrinsic pinning at lower fields. The interferences from twins and CuO layers become less pronounced with increasing impurity content or density of pointlike defects.

ACKNOWLEDGMENTS

This work was partly supported by the Bundesministerium für Forschung und Technologie under Grant No. 13N6177 and by Russian Fund for Fundamental Research, Grant No. 93-02-14768 and International Science Foundation, Grant No. MSW 300. A.A.Z. appreciates useful discussions with V. B. Geshkenbein.

APPENDIX

For the discrimination between the two current components in the geometry $B\|a,b$ the crystals were cut into a rectangular shape with a high aspect ratio parallel to the crystallographic axes. After the first measurement the sample was additionally cut parallel to the larger side ''a'' and measured again. For this reason we were able to measure Δm in $B\|a,b$ with the same aspect ratio a/c before and after the crystals were cut. Further in both parts for $B\|c$ the current densities j_1 before and j_2 after cutting were determined. The ratio j_1/j_2 vs field at $\phi=0$ is shown in Fig. 14 for crystal 3 as an example. As expected from the Bean model, assuming homogeneous current flow, this ratio is about 1. It increases towards the irreversibility line, partly due to the higher electric field at the surface of the larger crystal which results in higher current density values in the region of pronounced thermal relaxation where $E(j)$ curves become less steep. Thus in a wide field range j_1/j_2 vs B (dashed line in Fig. 14) is in fair agreement with the expected value 1 from the Bean model for the three cut crystals. This observation rejects also the presence of large scale inhomogeneities in the studied crystals. The value $\Delta m_1/\Delta m_2$ in $B\|a,b$ is expected from Eq. (2) to be equal to the ratio of the volumes $V_1/V_2=2.36$ in sample 3 (thin solid line in Fig. 14) because the aspect ratio is the same. The value $\Delta m_1/\Delta m_2$ (thick line in Fig. 14) shows normal behavior only at magnetic fields below 1 T. Above this field Δm_2 becomes considerably smaller than Δm_1 indicating an increase of $(j\|a,b)_2$ or/and a decrease of $(j\|c)_2$ with respect to the currents in the crystal before cutting. The same unusual behavior is observed in crystal 1 but not in crystal 2. The origin is not known, it may result from the same reasons as mentioned for the vanished PE in crystal 4, from cracks along the a,b plane or from changed properties of a surface barrier both introduced by the cutting process. The field at which $\Delta m_1/\Delta m_2$ starts to increase from its expected value corresponds in all crystals to the transition from the $\Delta m(\phi)$ peak to the dip behavior.

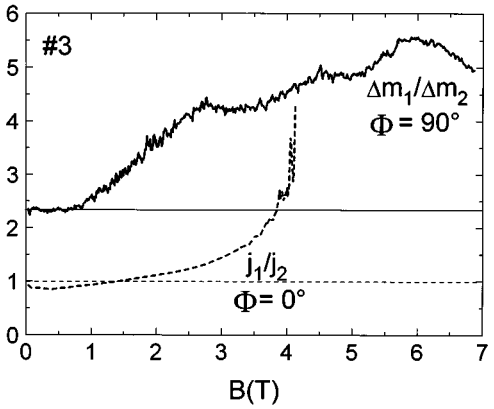

FIG. 14. The dashed line corresponds to the ratio of the current densities before the crystal was cut (j_1) and after (j_2) for the field B parallel to the c axis ($\phi=0°$). The bold line is the ratio of the hysteresis width Δm at $B\|a,b$ ($\phi=90°$) before and after cutting Δm_1 and Δm_2, respectively. The measurements are made at 77 K.

The measurements shown in Figs. 11(a)–11(d) were made on the original samples before cutting. After cutting the relative depth of the dip is more pronounced. For instance, crystal 1 becomes completely reversible at 77 K, $\phi=90°$ at higher fields. This may be interpreted with an easier channeling in crystals with smaller sizes or it may point to cracks introduced during cutting. Cracks parallel to the a,b plane would probably not influence $j\|a,b$ in $B\|a,b$ or $B\|c$ but decrease $j\|c$. We are not able to exclude this possibility but it becomes less probable from the absence of this phenomena in crystal 2. Furthermore the relative change of Δm for $B\|a,b$ before and after cutting is not present at low fields which would require cracks with a field-dependent current like in a junction. The ''lock-in'' oscillation becomes much less pronounced after cutting. This is in full agreement with the correlation of intrinsic pinning and ''lock-in'' oscillation to the current along a,b. This current shows the expected scaling behavior if the geometry of the crystals is changed, whereas the current along the c axis obviously does not scale with the geometry.

[1] M. Daeumling *et al.*, Nature (London) **346**, 332 (1990).
[2] S. N. Gordeev *et al.*, Phys. Rev. B **49**, 15 420 (1994).
[3] V. F. Solovjov *et al.*, Phys. Rev. B **50**, 13 724 (1994).
[4] L. Klein *et al.*, Phys. Rev. B **49**, 4403 (1994).
[5] A. A. Zhukov *et al.*, Phys. Rev. B **51**, 12 704 (1995).
[6] H. Küpfer *et al.*, Phys. Rev. B **52**, 7689 (1995).
[7] L. Vinnikov *et al.*, Solid State Commun. **67**, 421 (1988).
[8] W. K. Kwok *et al.*, Phys. Rev. Lett. **64**, 966 (1990).
[9] Th. Wolf *et al.*, J. Cryst. Growth **96**, 1010 (1989).
[10] D. J. L. Hong and D. M. Smith, J. Am. Ceram. Soc. **74**, 1751 (1991).
[11] S. Fleshler *et al.*, Phys. Rev. B **47**, 1448 (1993).
[12] F. Hellmann *et al.*, Phys. Rev. Lett. **68**, 867 (1992).
[13] G. Blatter *et al.*, Phys. Rev. Lett. **68**, 875 (1992).
[14] P. H. Kes *et al.*, Phys. Rev. Lett. **64**, 1063 (1990).
[15] G. Blatter *et al.*, Phys. Rev. B **43**, 7826 (1991).
[16] G. Blatter *et al.*, Rev. Mod. Phys. **66**, 1125 (1994).
[17] E. M. Gyorgy *et al.*, Appl. Phys. Lett. **55**, 283 (1989).
[18] V. V. Moshchalkov *et al.*, Superconductivity **2** (in Russian) 84 (1989).
[19] M. Oussena *et al.*, Phys. Rev. B **51**, 1389 (1995).

[20] A. A. Zhukov *et al.*, Phys. Rev. B **52**, R9871 (1995).
[21] W. K. Kwok *et al.*, Phys. Rev. Lett. **72**, 1092 (1994).
[22] D. S. Fisher *et al.*, Phys. Rev. B **43**, 130 (1991).
[23] M. C. Frischherz *et al.*, Supercond. Sci. Technol. **8**, 485 (1995).
[24] D. R. Nelson and V. M. Vinokur, Phys. Rev. Lett. **68**, 2398 (1992).
[25] D. R. Nelson and V. M. Vinokur, Phys. Rev. B **48**, 13 060 (1993).
[26] W. Jahn *et al.*, in Proceedings of Eucas 1995, the Second European Conference on Applied Superconductivity, Ediburgh, Scotland, edited by D. Dew-Hughes (Institute of Physics, London, 1995), p. 267.
[27] D. Lacey *et al.*, Supercond. Sci. Technol. **8**, 568 (1995).
[28] A. Gurevich, Phys. Rev. Lett. **65**, 3197 (1990).
[29] M. Tachiki and S. Takahashi, Solid State Commun. **70**, 291 (1989).
[30] V. G. Kogan and L. J. Campbell, Phys. Rev. Lett. **62**, 1552 (1989).
[31] B. I. Ivlev *et al.*, J. Low Temp. Phys. **80**, 187 (1990).
[32] M. Oussena *et al.*, Phys. Rev. Lett. **72**, 3606 (1994).